Multiple pH-Induced Morphological Changes in Aggregates of Polystyrene-*block*-poly(4-vinylpyridine) in DMF/H_2O Mixtures

Hongwei Shen, Lifeng Zhang, and Adi Eisenberg*

Contribution from the Department of Chemistry, McGill University, 801 Sherbrooke Street West, Montreal, Quebec, Canada H3A 2K6

Received October 22, 1998

Abstract: Multiple changes in the aggregate morphologies of polystyrene-*block*-poly(4-vinylpyridine) (PS-*b*-P4VP) diblocks have been observed as a function of the apparent pH (pH*) in DMF/H_2O mixtures. The pH* changes were induced by adding HCl (in the concentration range 400 nM−20 mM) or NaOH (100 nM−20 mM). On the acid side, as the pH* increases from 7 (20 mM HCl) to 12.3 (the pH* of the original polymer solution without any additional microions), the aggregate morphology changes from large compound micelles (LCMs) to a mixture of spheres, rods, and vesicles (pH* = 8), to spheres (pH* = 8.4), to rods (pH* = 11.8), and then back to spheres (pH* = 12.3). In the presence of NaOH, as the pH* increases from 12.3 to 18 (20 mM NaOH), the morphology changes to rods (pH* = 12.6), then back to spheres again (pH* = 17.5), and finally to a mixture of spheres, rods, lamellae, and vesicles (pH* = 18). This level of morphological complexity as a function of pH* is unprecedented. The reasons for the behavior can be ascribed to the amphiprotic nature of P4VP in DMF. The addition of either an acid or a base introduces ionic groups into the corona chains. Thus electrostatic repulsion is introduced and the aggregate morphology changes generally in the direction of bilayers to spheres. However, due to the existence of multiple equilibria, some of the added microions are free, which decreases the steric−solvation interaction and decreases the electrostatic repulsion by shielding. This decrease in the corona repulsion tends to decrease the coil dimensions in the corona. As a result, the morphology is driven in the direction of spheres to bilayers. Therefore, a competition between unshielded electrostatic repulsion and shielding coupled with a decrease of the steric−solvation interaction is induced. At relatively low concentrations, the decrease of the steric−solvation interaction dominates, while at relatively high concentrations, the shielding dominates. In intermediate regions, the unshielded electrostatic repulsion is dominant. The morphological transitions induced by extremely low concentrations of HCl or NaOH (100 nM−1 μM) are very surprising. The effect of a neutral salt (NaCl) on the neutral copolymer and the effect of pH* on a quaternized copolymer were also explored.

1. Introduction

Complex phase behavior has been observed for block copolymers in bulk and in concentrated solutions.[1,2] Recently, aggregates of multiple morphologies were also observed in dilute block copolymer solutions, where spheres, rods, lamellae, vesicles, and large compound micelles (LCMs) were seen, among others.[3−9] Several systems have been investigated so far, including polystyrene-*block*-poly(acrylic acid) (PS-*b*-PAA) and polystyrene-*block*-poly(ethylene oxide) (PS-*b*-PEO) in aqueous solutions,[3−7] polystyrene-*block*-poly(2-vinylpyridine) (PS-*b*-P2VP) in toluene,[8] and polyisoprene-*block*-poly(2-cinnamoylethyl methacrylate) (PI-*b*-PCEMA) and PS-*b*-PCEMA in organic solvents.[9]

In the case of PS-based block copolymers (i.e., PS-*b*-PAA, PS-*b*-PEO, etc.), PS is the hydrophobic core-forming block, while PAA, PEO, etc. are the hydrophilic corona-forming blocks.[3−7] Due to the high hydrophobicity of the PS block, the aggregates are prepared by dissolving block copolymers in a common solvent (e.g., DMF, dioxane, THF), followed by the addition of a precipitant for the core-forming block (i.e., deionized water) and dialysis to remove the organic solvents. In the course of dialysis, the aggregates become frozen and can be studied by TEM.

It has been found that the aggregate morphology is controlled mainly by a force balance involving three parameters.[4] These parameters include the stretching (deformation) of the core-forming blocks in the core, the repulsive interaction among the corona chains, and the interfacial tension at the core−corona interface. Thus, many factors may affect the final morphologies of the aggregates because of their effects on the three parameters. Among these factors, the most important are the nature of the core-forming block and the corona-forming block, the composi-

* To whom correspondence should be addressed. E-mail: eisenber@omc.lan.mcgill.ca.

(1) Bates, F. S.; Fredrickson, G. H. *Annu. Rev. Phys. Chem.* **1990**, *41*, 525.

(2) Wanka, G.; Hoffmann, H.; Ulbricht, W. *Macromolecules* **1994**, *27*, 4145. Alexandridis, P.; Holmqvist, P.; Lindman, B. *Colloids Surf., A* **1997**, *130*, 3.

(3) Zhang, L.; Eisenberg, A. *Science* **1995**, *268*, 1728; *J. Am. Chem. Soc.* **1996**, *118*, 3168.

(4) Zhang, L.; Yu, K.; Eisenberg, A. *Science* **1996**, *272*, 1777. Zhang, L.; Eisenberg, A. *Macromolecules* **1996**, *29*, 8805.

(5) Yu, K.; Eisenberg, A. *Macromolecules* **1996**, *29*, 6359. Yu, K.; Zhang, L.; Eisenberg, A. *Langmuir* **1996**, *12*, 5980. Zhang, L.; Bartels, C.; Yu, Y.; Shen, H.; Eisenberg, A. *Phys. Rev. Lett.* **1997**, *79*, 5034.

(6) Zhang, L.; Shen, H.; Eisenberg, A. *Macromolecules* **1997**, *30*, 1001.

(7) Yu, Y.; Eisenberg, A. *J. Am. Chem. Soc.* **1997**, *119*, 8383. Yu, Y.; Zhang, L.; Eisenberg, A. *Macromolecules* **1998**, *31*, 1144.

(8) Spatz, J. P.; Mössmer, S.; Möller, M. *Angew. Chem., Int. Ed. Engl.* **1996**, *35*, 1510. Spatz, J. P.; Sheiko, S.; Möller, M. *Macromolecules* **1996**, *29*, 3220.

(9) Ding, J.; Liu, G. *Macromolecules* **1997**, *30*, 655. Ding, J.; Liu, G.; Yang, M. *Polymer* **1997**, *38*, 5497.

10.1021/ja983712m CCC: $18.00
Published on Web 03/11/1999

tion of the copolymer, the nature of the common solvent and the precipitant, and the presence and nature of any additives, such as ionic groups.

The nature of the core-forming block affects the aggregate morphology mainly through its effect on the interfacial tension at the core−corona interface, which increases with increasing hydrophobicity of the core-forming block. The length of the corona-forming block influences the aggregate morphology through its effect on the repulsive interaction among the corona chains. Thus, with increasing corona block length, the aggregates may change from vesicles to rods or even spheres.[3] Solvents also play an important role in the aggregation process. The common solvent mainly modifies the degree of the stretching of the core-forming block in the core through a change of the solvent content in the core and a change in the aggregation number, although the corona repulsion and the interfacial tension may change at the same time. As the solvent changes from DMF to THF and then to dioxane, the degree of the stretching increases and the aggregates change from spheres to rods and then to vesicles.[7]

The addition of some microions has a very important and complicated effect on the aggregation behavior through its influence on the repulsive interaction among corona chains. For example, in the case of PS_{410}-*b*-PAA_{25} in DMF/water mixtures, the addition of NaCl to a total concentration of 11 mM changes the aggregate morphologies from spheres to vesicles by screening the electrostatic repulsion among corona chains;[4] the presence of HCl at a concentration of 240 μM changes spherical aggregates to vesicles through the protonation of the PAA block;[4] a concentration of 140 μM of Ca_2Cl_2 has the same effect as a result of Ca^{2+} bridging.[4] Upon addition of NaOH to a total concentration of 28 μM, the morphologies of the aggregates of PS_{410}-*b*-PAA_{13} change from vesicles to spheres due to the increase of the electrostatic repulsion accompanying the neutralization of the PAA block.[4] The above examples clearly show that the effects of the microions can differ significantly depending on detailed interactions between added microions and the corona chains.

The aggregation behavior of PVP (including P4VP and P2VP) based copolymers has received some attention recently. Selb and Gallot reviewed the aggregation behavior of quaternized PS-*b*-P4VP copolymers in water/methanol systems, among others.[10] Several other groups investigated PS-*b*-PVP in toluene, where reverse micelles are formed.[8,11,12] The only pH-related study was performed by Munk, Webber, and co-workers on the copolymer P2VP-*b*-PEO in aqueous media.[13] In their study, however, P2VP was the core-forming block. With increasing pH, the degree of the protonation of the P2VP decreases, and thus its solubility in water also decreases. Micelles appear above a pH of 5.[13]

The polymer PVP is generally a base, as shown in the above study. However, in a basic solvent such as DMF, the α-H of VP may show some acidity through its special resonance structures.[14] Thus, PVP may show either acidic or basic properties in a basic solvent. When PVP is the corona-forming block, with changing pH, the nature of the corona will change from cationic to nonionic or to anionic. Thus, the aggregation behavior of copolymers with a PVP corona will change significantly. However, in the systems mentioned above, amphiprotic properties were not observed since PVP was either quaternized and in the corona or nonquaternized and in the core. Also, the studies mentioned above dealt with spherical micelles.

In the present paper, we describe the pH effect on the aggregate morphology of the copolymer PS_{310}-*b*-$P4VP_{58}$ in DMF induced by the addition of H_2O. From the previous studies in the PS-*b*-PAA systems,[4] one can expect a straightforward effect of pH on the aggregate morphology. As the pH increases, the morphology will change monotonically from LCMs to vesicles, then to rods, and finally to spheres. In contrast to the above behavior, the present study of a PS-*b*-P4VP copolymer shows that as the pH increases, the morphology changes from LCMs to spheres, then to rods, back to spheres, then to rods again, back again to spheres, and finally to a mixture of various morphologies. This unusual behavior can be attributed to the amphiprotic properties of P4VP. Because DMF is a basic solvent, the hydrophilic block, P4VP, can be modified to cationic or anionic by addition of HCl or NaOH. Thus electrostatic repulsion among the corona is introduced. In some concentration ranges, shielding is involved in the force balance in addition to the decrease of the steric−solvation interaction. Thus a complex morphological behavior is induced due to the competition between the electrostatic repulsion introduced by addition of acid or base and the shielding along with the decrease of the steric−solvation interaction. In a parallel investigation, the effect of a neutral salt (NaCl) on the copolymer and the effect of pH on the quaternized copolymer (which is no longer basic) were also examined.

2. Experimental Section

2.1. Block Copolymers. The polystyrene-*block*-poly(4-vinylpyridine) (PS-*b*-P4VP) diblock copolymers were synthesized by sequential anionic polymerization of styrene followed by 4-vinylpyridine (4VP).[15] *sec*-Butyllithium was used as the initiator. The polymerization was carried out in tetrahydrofuran (THF) at −78 °C under nitrogen. After the polystyrene block was formed, an aliquot of the reaction mixture was withdrawn for characterization. Subsequently, a series of diblock copolymers with the same polystyrene block length were obtained by withdrawing aliquots of the mixtures after each 4VP monomer addition.

The degrees of polymerization of the PS blocks and the polydispersities of the homopolymer and of the diblocks were determined by gel permeation chromatography (GPC). The homopolystyrene and all the diblock copolymers in the form of 4VP gave one sharp GPC peak. The precise degrees of polymerization of the P4VP blocks cannot be determined by GPC due to some adsorption of the P4VP block in the GPC column, which introduces a systematic error into the retention time measurements. The polydispersities determined by GPC for the diblocks containing P4VP should be broader than the real polydispersities and thus can be considered only as the upper limits. NMR was used to measure the degree of polymerization of the P4VP blocks by reference to the PS content.[15]

The P4VP blocks of the copolymers were quaternized to their salt (ionic) forms in THF using methyl iodide as the quaternizing agent. IR was used to examine the degree of quaternization. The quaternization was taken to be complete because no peak was seen at 1414 cm^{-1}. A detailed description of the procedures can be found elsewhere.[15] The polymers are identified by giving the degree of polymerization as subscripts. For example, PS_{310}-*b*-$P4VP_{58}$ represents a diblock copolymer containing 310 styrene repeat units and 58 4-vinylpyridine repeat units (number average). The nonquaternized copolymer PS_{310}-*b*-$P4VP_{58}$ (PI = 1.07) and the quaternized copolymer PS_{600}-*b*-$P4VPMeI_{37}$ (PI = 1.05) were used in this study. PI is the polydispersity index, which is defined

(10) Selb, J.; Gallot, Y. In *Developments in block copolymers*; Goodman, I., Ed.; Applied Science Publishers: London, 1985; Vol. 2, p 27.
(11) Förster, S.; Zisenis, M.; Wenz, E.; Antonietti, M. *J. Chem. Phys.* **1996**, *104*, 9956.
(12) Calderara, F.; Riess, G. *Macromol. Chem. Phys.* **1996**, *197*, 2115.
(13) Martin, T. J.; Procházka, K.; Munk, P.; Webber, S. E. *Macromolecules* **1996**, *29*, 6071.
(14) Streitwieser, A., Jr. *Introduction to Organic Chemistry*, 4th ed.; Macmillan: New York, 1992; p 1116.
(15) Zhu, J.; Eisenberg, A.; Lennox, R. B. *J. Am. Chem. Soc.* **1991**, *113*, 5583.

as the ratio of the weight average molecular weight (M_w) to the number average molecular weight (M_n).

2.2. pH Measurements and UV−Visible Spectroscopy. The pH measurements were performed using a Corning pH meter, model 245. Because the solutions used in the present study were nonaqueous (in DMF), a millivolt scale was employed rather than the direct pH scale. The millivolt scale was calibrated with standard pH buffers (pH 4.00, 7.00, and 10.00), as well as 10.0 M HCl and 10.0 M NaOH aqueous solutions. Thus, the measured pH values do not have the same meaning as those in water and are reported as apparent pH, pH*, according to previous usage.[16] The pH* of the polymer solutions was measured in pure DMF or in DMF in the presence of ca. 1.0 wt % water for the samples involving additional microions. The addition of 10 wt % water in DMF only decreases the pH* from 11.7 to 11.4. Thus, the addition of water does not change the pH* considerably.

UV−visible spectroscopy was performed on an 8452A diode array spectrophotometer (Hewlett-Packard) using HP 89531A MS-DOS UV/VIS Operation Software. Spectra were recorded from 200 to 800 nm using DMF as a reference.

2.3. Preparation of the Aggregates. Diblock copolymers were first dissolved in DMF, which is a common solvent for both blocks in the molecular weight ranges used here. The initial copolymer concentration in DMF was 1.0 wt %. For samples involving the addition of microions, a calculated amount of microions in aqueous solutions (ca. 1.0 wt % of the total solution) was added to the copolymer solutions and the mixed solutions were kept overnight to reach equilibrium. Then, after pH* measurements, deionized water was added to the copolymer solutions at a rate of 0.2 wt %/30 s with stirring. The appearance of cloudiness in the solution indicated that aggregation had taken place. Aggregation generally occurs at 3−5 wt % water, depending on the composition of the copolymers and the presence of microions. On the basis of the evidence from a previous paper, the aggregates become kinetically frozen at ca. 10 wt % of water.[6] Thus, the polymer concentration, the pH*, and the microion concentration are nearly constant during the whole aggregation process. We added 35 wt % water before the dialysis, which was used to remove all the DMF from the solutions. At such high water contents, the aggregates do not undergo any changes during dialysis.

Although the P4VP block is not soluble in pure water, it is soluble in DMF solutions containing up to 50 wt % water and is also soluble in water below a pH of 5. Thus, for dialysis of the solutions of the aggregates of PS-*b*-P4VP, the pH of the distilled water was adjusted to 4 to keep the colloid solutions from precipitating. However, even without the pH adjustment, the aggregates that precipitate during the dialysis process can be readily redissolved in acidic water. It should be stressed that the overall morphology and the average diameter are identical within experimental error with and without the pH adjustment. Thus, the adjustment does not influence the experimental results.

2.4. Transmission Electron Microscopy. Transmission electron microscopy (TEM) was performed on a Phillips EM400 microscope operating at an acceleration voltage of 80 kV. For the observation of the size and distribution of the aggregates, samples were deposited from dilute aqueous solutions (ca. 0.05 wt %) onto EM copper grids, which had been precoated with a thin film of Formvar (J. B. EM Services Inc.) and then coated with carbon. Water was evaporated at atmospheric pressure and room temperature. The grids were shadowed with a palladium/platinum alloy at an angle of 35°. The sizes of aggregates were measured directly from the prints of the microscope negatives after calibration using a standard PS latex.

3. Results and Discussion

This section is divided into four parts. The first part discusses the effect of pH* on the aggregate morphology of a nonquaternized (nonionic) diblock, PS_{310}-*b*-$P4VP_{58}$, in DMF induced by the addition of H_2O. The second part is devoted to the effect of NaCl on the aggregate morphology of PS_{310}-*b*-$P4VP_{58}$. The pH* effect on the aggregation behavior of a quaternized (ionic) diblock, PS_{600}-*b*-$P4VPMeI_{37}$, in DMF induced by the addition of H_2O is presented in part 3. Finally, the competition of the corona repulsive forces underlying the complex phenomena seen here is described qualitatively in some detail.

Since the present study deals with the effect of added microions on the aggregate morphology, the addition of microions should mainly affect corona−corona repulsive interactions. At present, however, the repulsive interactions among corona chains are still too complex for a quantitative description. For nonionic corona chains, these interactions generally include a steric contribution and a solvation contribution.[17] Because both the steric and the solvation interactions are short-range forces, it is impossible to separate the contributions arising from pure steric forces and pure solvation effects.[17] Thus, these two interactions together are generally referred to as the "steric−solvation interaction". If the corona chains are charged, the repulsive interactions also contain an electrostatic repulsive contribution in addition of the steric−solvation interaction. The electrostatic repulsive interaction is a long-range force and is thus much more important at relatively long distances.

In the materials of the present study, the corona chains may be either ionic or nonionic. The nature of the repulsive interactions will therefore change correspondingly. However, the total minimum energy (including the attractive interfacial tension and the repulsive interactions among corona chains) at the onset of the microphase separation is proportional to the optimized surface area per corona chain.[17] Also, the attractive interfacial tension is proportional to the surface area per corona chain.[17] Therefore, the attractive force is proportional to the optimized surface area per corona chain under equilibrium conditions. Thus, independent of the nature of the corona chains and the origin of the repulsive interactions, the overall repulsive interaction (force) among corona chains at the onset of aggregation is proportional to the optimized surface area per corona chain. The optimized surface area per corona chain will be used to represent the overall repulsive interaction in the following discussion. When multiple morphologies are present, weight averages of the numerical values of the repulsive interactions are taken.

3.1. Effect of pH* on the Aggregate Morphology of PS_{310}-*b*-$P4VP_{58}$. 3.1.1. Acid (HCl) Effect. The effect of HCl on the morphology of the aggregates of the copolymer PS_{310}-*b*-$P4VP_{58}$ formed in DMF by addition of H_2O is shown in Figure 1. Figure 1A shows spherical aggregates (the average radius, *r*, is 22 nm) of the copolymer in a solution without any added microions, in which the measured pH* in DMF is 12.3. Upon addition of HCl to a final concentration of 40 μM (at which the molar ratio of HCl/4VP, *R*, is 0.003), the pH* reaches the value of 11.8 and most of the aggregates become rodlike (Figure 1B), with diameters similar to those of the spheres in Figure 1A. When the HCl concentration increases to 5.0 mM (Figure 1C), the morphology of aggregates changes back to spheres with smaller radii ($r = 19$ nm) than those in Figure 1A. At this point, the *R* value is 0.36, much higher than that for the sample shown in Figure 1B, while the pH* is 8.4, much lower. When the HCl concentration reaches 10 mM ($R = 0.71$ and pH* = 8.0), the aggregates change their morphologies from spheres to a mixture of spheres, rods, and vesicles, as shown in Figure 1D. At a still higher HCl concentration (20 mM, $R = 1.43$, and pH* = 7.0), large spheres appear, as shown in Figure 1E. This indicates that the aggregates undergo a secondary aggregation and internal reorganization and form LCMs.

(16) Dean, J. A. *Analytical Chemistry Handbook*, 4th ed.; McGraw-Hill Inc: New York, 1995; pp 3.53, 14.31.

(17) Israelachivili, J. N. *Intermolecular and Surface Forces*, 2nd ed.; Academic Press: London, San Diego, 1992.

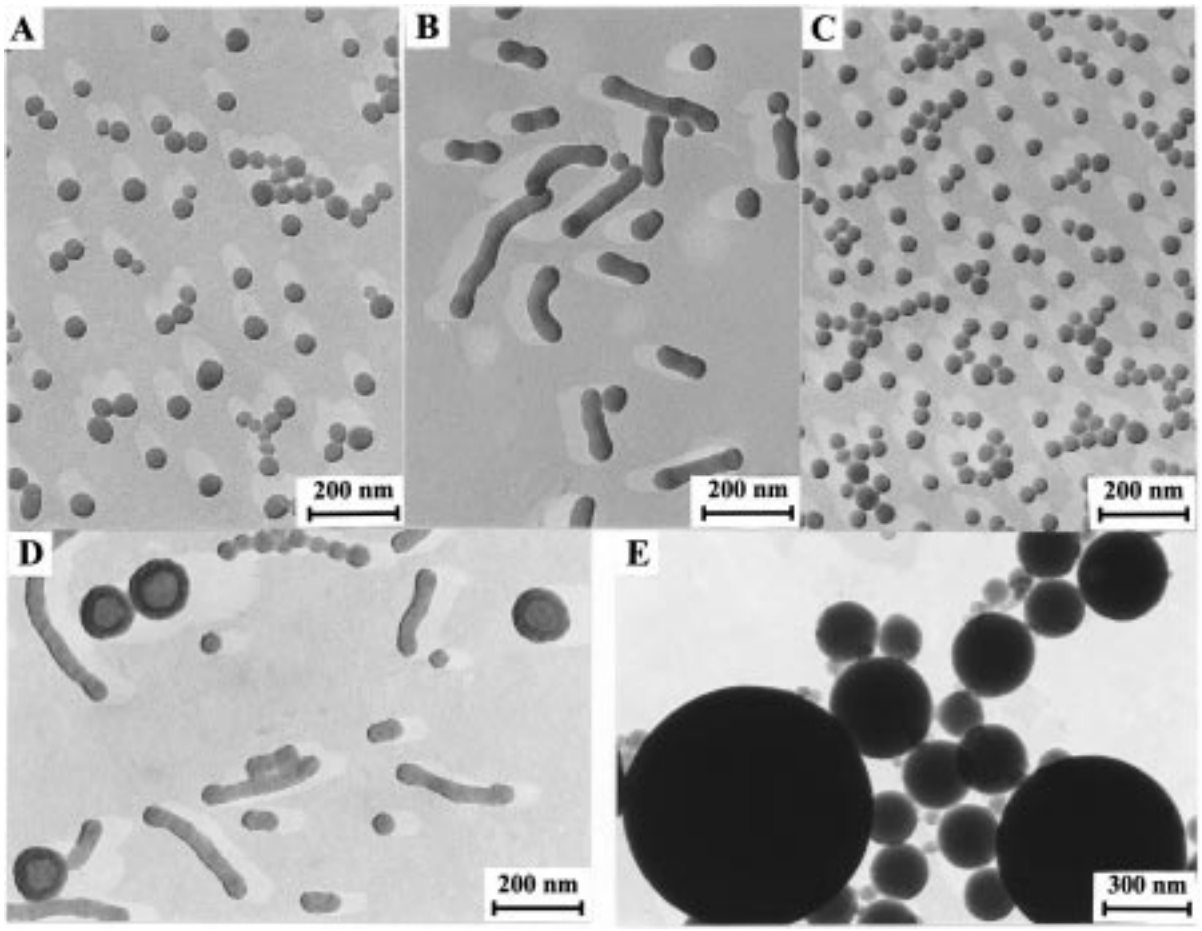

Figure 1. Effect of HCl on the aggregate morphology of copolymer PS_{310}-*b*-$P4VP_{58}$: (A) without any added microions, pH* = 12.3, α = 0; (B) 40 μM (R = 0.003), pH* = 11.8, α = 0.26%; (C) 5.0 mM (R = 0.36), pH* = 8.4, α = 32%; (D) 10 mM (R = 0.71), pH* = 8.0, α = 60%; (E) 20 mM (R = 1.43), pH* = 7.0, α = 88%.

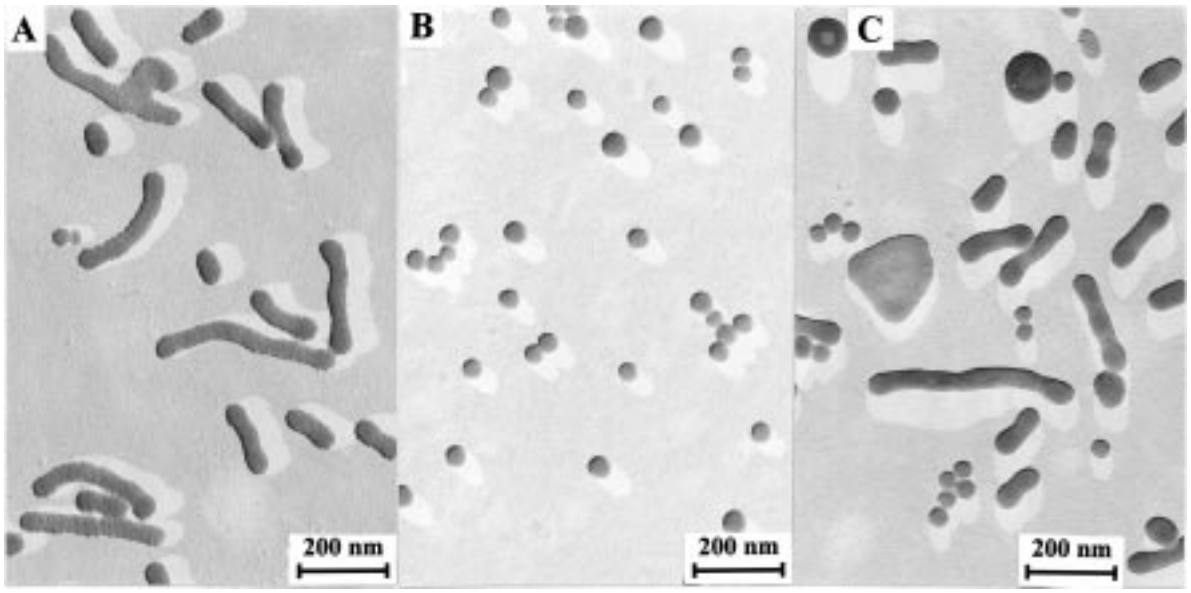

Figure 2. Effect of NaOH on the aggregate morphology of copolymer PS_{310}-*b*-$P4VP_{58}$: (A) 400 nM ($R = 3 \times 10^{-5}$), pH* = 12.6, α ≈ 0; (B) 5.0 mM (R = 0.36), pH* = 17.5, α = 2.5%; (C) 20 mM (R = 1.43), pH* = 18.0, α = 9.5%.

3.1.2. Base (NaOH) Effect. Figure 2 shows the effect of NaOH on the aggregate morphology of the same copolymer. The starting point is again Figure 1A. At a NaOH concentration of 400 nM ($R = 3 \times 10^{-5}$ and pH* = 12.6), the aggregates are mainly rodlike, as shown in Figure 2A. The NaOH concentration at this point is extremely low, with only 1 NaOH unit per 30 000 4VP units or 9 NaOH units per aggregate, yet most of the aggregates have become rodlike. When the NaOH concentration increases to 5.0 mM (R = 0.36 and pH* = 17.5), the morphologies change back to spheres (r = 21 nm), as shown in Figure 2B. With a further increase of the NaOH concentration to 20 mM (R = 1.43 and pH* = 18.0), the aggregates again

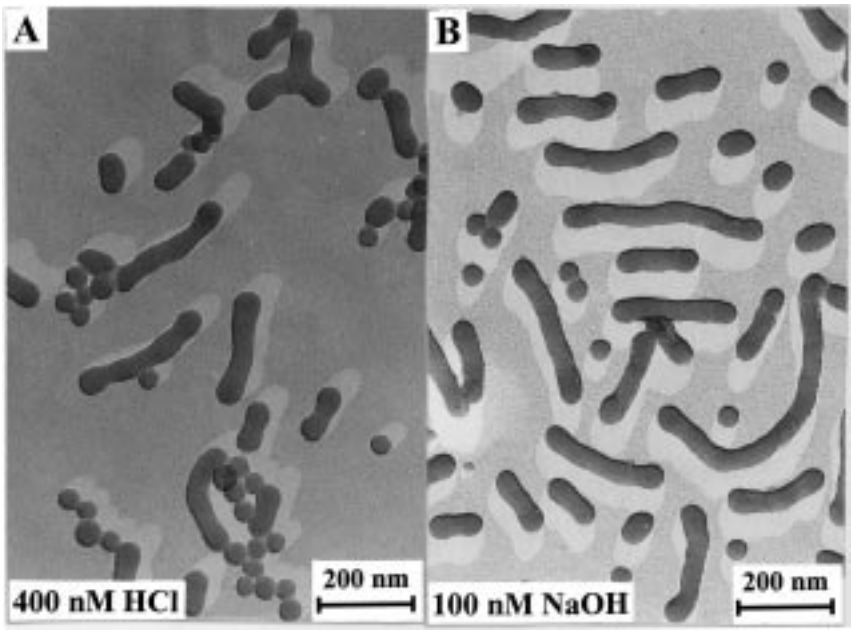

Figure 3. Aggregates of copolymer PS_{310}-*b*-$P4VP_{58}$ at extremely low concentrations of microions: (A) 400 nM HCl, 3 HCl units per aggregate or $R = 3 \times 10^{-5}$; (B) 100 nM NaOH, 1 NaOH unit per aggregate or $R = 7 \times 10^{-6}$.

change their morphologies from spheres to a mixture of spheres, rods, lamellae, and even vesicles. Figure 2C shows this mixture of morphologies. Due to the limited solubility of NaOH in DMF, higher NaOH concentrations are not accessible.

3.1.3. Aggregate Morphologies at the Lowest Concentrations of HCl and NaOH. Figure 3 shows the aggregates of the same copolymer obtained at the lowest contents of acid and base. On the acid side (the starting point is Figure 1A, pure spheres), an HCl concentration of 400 nM induces the appearance of rods, as shown in Figure 3A. At that concentration, the ratio of HCl units to 4VP units is 1 to 30 000, corresponding, on average, to 3 HCl units per aggregate. On the base side, the effect is even more dramatic. An NaOH concentration of 100 nM (140 000 4VP units per NaOH unit or 1 unit of NaOH per aggregate) can induce the formation of rods, as seen in Figure 3B. The concentrations used here are far lower than the lowest concentration used before (28 μM NaOH).[4] It has been generally recognized that the balance of forces responsible for morphological changes in small molecule surfactants or block copolymers is very delicate. In the view of very small concentration changes, which are now seen to induce morphological changes, this balance of forces seems to be much more delicate than has been appreciated before.[4]

3.1.4. Semiquantitative Considerations. Figures 1−3 show a complicated pH effect on the morphology of aggregates. As the pH* increases from 7 to 12.3 (the neutral pH*) and then to 18, the aggregates go through morphological transitions from LCMs to a mixture of various morphologies, to small spheres, to rods, back to small spheres at the neutral pH*, back to rodlike aggregates, then to small spherical aggregates again, and finally to a mixture of multiple morphologies. A semiquantitative discussion of this pH* effect in terms of repulsive interactions among corona chains follows.

3.1.4.1. Amphiprotic Properties of P4VP in DMF. It is well-known that P4VP is a weak base due to the presence of the unprotonated N on the pyridine ring. However, it may also act as an acid. The α-H of P4VP can provide the proton because the resulting product can be stabilized by the pyridine ring through several resonance structures.[14] In aqueous solutions, however, P4VP cannot show its acidity due to its extremely

Scheme 1. Amphiprotic Properties of P4VP in DMF

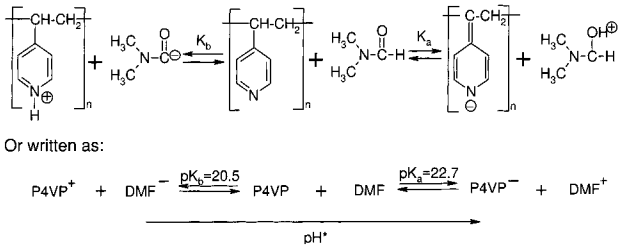

low acidic dissociation constant (the estimated pK_a and pK_b values of pyridine are ca. 20 and ca. 9, respectively[14]). In a basic solvent (i.e., DMF), the relative acidity of the α-H increases and the relative basicity of the N decreases. Thus, in this particular system, P4VP can show both acidic and basic properties, as indicated in Scheme 1. Since the pH* value is 11.7 for pure DMF and 12.3 for the copolymer solution, overall P4VP is a weak base and has relatively low acidic dissociation (pK_b is ca. 20.5 and pK_a is ca. 22.7).

As shown in Scheme 1 (right side), after release of the α-H, the β-H of P4VP changes to a new "α′-H". However, the new α′-H cannot show its acidity in DMF for the same reason that the α-H of P4VP cannot show its acidity in H_2O. Thus, in DMF solutions, the P4VP block can only release its α-H. Because of the properties described above, P4VP can be neutralized by an acid to form cationic blocks and by a base to form anionic blocks. With increasing pH* (starting from a pH* far below 12.3), the P4VP blocks should vary from cationic ($P4VP^+$) to nonionic (P4VP) and then to anionic ($P4VP^-$). It should be noted that, in DMF, any acid species would be present in the form of DMF^+ instead of H_3O^+ in water; similar considerations apply to bases (DMF^- instead of OH^-).

3.1.4.2. Estimation of the Degree of Ionization of P4VP in DMF upon Addition of an Acid or a Base. The electrostatic repulsive interaction introduced by the addition of HCl or NaOH is obviously associated with the degree of ionization of the corona chains, which can be used to estimate the strength of the electrostatic repulsion. The ionization of salts, strong acids, and strong bases can be complete upon dissolution in DMF

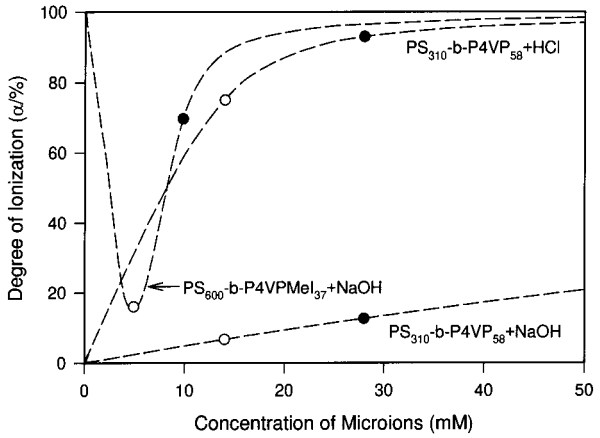

Figure 4. Plots of the estimated degree of ionization against the concentration of HCl or NaOH for copolymers PS_{310}-*b*-$P4VP_{58}$ and PS_{600}-*b*-$P4VPMeI_{37}$. Open circles indicate a molar ratio of HCl or NaOH to 4VP units (R) of 1. Closed circles indicate a ratio R of 2.

because of the high dielectric constant of the solvent ($\epsilon = 38.2$ at 20 °C).[18]

The dissociation constant of DMF together with the acidic and the basic dissociation constants of P4VP can be determined approximately from pH measurements. From these dissociation constants, the degree of ionization can be estimated. For example, in the case of the addition of HCl to the copolymer solution, an equilibrium is operative (the concentrations of the relevant species are given below the symbols):

$$\underset{(1-\alpha)C}{\text{P4VP}} + \underset{([\text{DMF}^+]-\alpha C)}{\text{DMF}^+} \overset{K_b/K_{DMF}}{\rightleftharpoons} \underset{\alpha C}{\text{P4VP}^+} + \text{DMF}$$

α represents the degree of ionization of the P4VP, C is the concentration of 4VP units in moles per liter, $[DMF^+]$ is equal to the HCl concentration in moles per liter, and K_{DMF} and K_b are the dissociation constant of DMF and the basic dissociation constant of P4VP, respectively. The degree of ionization can then be calculated from

$$(1-\alpha)([\text{DMF}^+]-\alpha C) = \alpha K_{DMF}/K_b \quad (1)$$

Similar principles apply to the addition of NaOH to nonquaternized and quaternized P4VP solutions. The degrees of ionization can also be calculated for those situations.

Figure 4 shows the plot of the calculated degrees of ionization against the concentration of HCl or NaOH. Because all added microions are monovalent, the concentration is used directly for the plot rather than the ionic strength. On the graph, open circles are used for conditions in which the molar ratio of HCl or NaOH units to 4VP units (R) is 1; closed circles indicate that R is 2. From the curves for $PS_{310}-P4VP_{58}$, it is clear that the degree of ionization increases much faster with the addition of HCl than with the addition of NaOH. In fact, when R is 1, the degree of ionization for the addition of HCl is ca. 75%, while for addition of NaOH, it is below 10%. Clearly, not all of the added HCl or NaOH is used to convert P4VP to $P4VP^+$ or $P4VP^-$, and thus some of the HCl or NaOH is unreacted. The difference in the degree of ionization and in the concentration of free microions should affect the electrostatic repulsion and the steric−solvation interaction.

(18) Lide, D. R. *CRC Handbook of Chemistry and Physics*, 77th ed.; CRC Press: New York, 1996; pp 8−100.

3.1.4.3. Estimation of the Aggregation Number and the Surface Area per Corona Chain. Since the corona repulsion is associated with the surface area per corona chain,[17] it is very helpful for the present discussion to estimate the aggregation number and then the magnitude of the surface area per corona chain. The aggregation number can be estimated from TEM pictures by assuming that the density of the observed aggregates is homogeneous and equal to the value of PS in the solid state. The surface area per corona chain can be determined from the size of the aggregates by assuming that there is a smooth core−corona interface. Thus, the aggregation number (N_{agg}) and the surface area per corona chain (A_c, nm^2/chain) can be given by the following equations.

For spherical aggregates

$$N_{agg} = (4/3)\pi r^3/VN \quad (2)$$

$$A_c = 4\pi r^2/N_{agg} = 3VN/r \quad (3)$$

V is the volume of a PS repeat unit (0.167 nm^3), N is the total number of repeat units (PS and P4VP), and r is the radius of a sphere in nm. For small spheres (primary aggregates), eqs 2 and 3 can give reliable results.[3] However, for the large spheres (LCMs), some errors are introduced because some of the corona chains are in the core. Nevertheless, this estimation can give a relative magnitude for the aggregation number and the average surface area per corona chain.

For rodlike aggregates

$$N_{agg} = [(4/3)\pi r^3 + \pi r^2(L-2r)]/VN \quad (4)$$

$$A_c = [(4\pi r^2 + 2\pi r(L-2r)]/N_{agg} = 6LVN/(3Lr-2r^2) \quad (5)$$

L is the length of a rod in nm, and the remaining symbols are the same as those for spherical aggregates. Additional assumptions made in the derivations are that the end caps of the rod are perfect hemispheres, the radii of the rod are constant over the whole length, and the end caps and the middle of the rod have the same surface area per corona chain.

For vesicles

$$N_{agg} = (4/3)\pi({r_{out}}^3 - {r_{in}}^3)/VN \quad (6)$$

$$A_c = 4\pi({r_{out}}^2 + {r_{in}}^2)/N_{agg} = 3VN({r_{out}}^2 + {r_{in}}^2)/({r_{out}}^3 - {r_{in}}^3) \quad (7)$$

r_{out} is the outside radius and r_{in} is the inside radius of a vesicle in nm, and the rest of the symbols are the same as those for spheres. It is further assumed that the thickness of the vesicle is uniform and that the surface area per corona chain is the same on the inside and outside of the vesicle.

For circular lamellae, the two parameters can be approximately determined by

$$N_{agg} = 2\pi r^2 h/VN \quad (8)$$

$$A_c = 4\pi r^2/N_{agg} = VN/h \quad (9)$$

r is the radius and h is the thickness of a lamella in nm; again the rest of the symbols are the same as above. In addition, it is assumed that the lamella is a perfect homogeneous disk and that the surface area per corona chain is the same on the edges and in the middle of the lamella.

The aggregation number and the surface area per corona chain for rods, vesicles, lamellae, and LCMs should be considered as

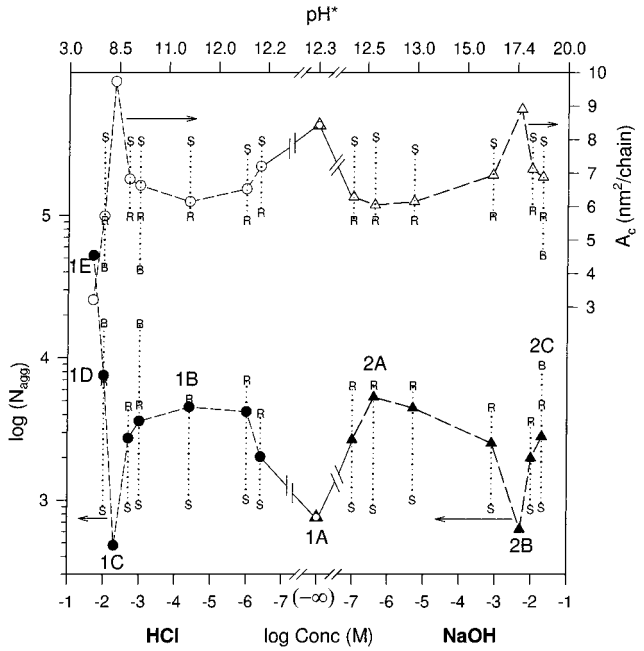

Figure 5. Plots of the logarithm of the average aggregation number (bottom plot and left axis label) and the average surface area per corona chain (top plot and right axis label) against the logarithm of the microion concentration in the solutions for aggregates of PS_{310}-*b*-$P4VP_{58}$. The upper scale gives the approximate value of pH*. The $-\infty$ on the log Conc scale corresponds to a zero microion concentration and a pH* of 12.3. The effect of HCl is graphed on the left side (circles), while the effect of NaOH is graphed on the right side (triangles). The labels on the graph indicate the points that represent TEM pictures shown in the figures with the same labels. For example, point 1A represents the picture shown in Figure 1A. The small letters, S, R, and B, connected with points represent spheres, rods, and bilayers (including vesicles and lamellae). The points are the averages for the aggregates and should be considered as rough estimates, except those for primary spheres (points 1C, 1A and 2B).

semiquantitative estimates because many assumptions have been made. However, the values for small spheres are reliable.[3] Using eqs 2−9, the aggregation number and the surface area per corona chain can be estimated for the regularly shaped aggregates. The average aggregation number and the average surface area per corona chain are used in the discussion. In cases where multiple morphologies coexist, averages are obtained, but they obviously do not have the well-defined meaning that they do for aggregates of a single morphology. However, these averages do indicate the relative changes for various conditions and reflect relative populations of the various types of aggregates. The average surface area per corona chain can be used to represent the overall repulsion among corona chains, considering it as the optimized surface area per corona chain.

3.1.4.4. Reasons for the pH* Effect on the Aggregate Morphology. Figure 5 gives the graph of the logarithm of the average aggregation number (lower curve, left axis) and the average surface area per corona chain (upper curve, right axis) against the logarithm of the microion concentration in the solutions. The approximate value of pH* is given on the upper scale. The $-\infty$ in the middle of the log Conc scale corresponds to a zero microion concentration at a pH* of 12.3. The effect of HCl is graphed on the left side (circles), while the effect of NaOH is graphed on the right side (triangles). The labels on the graph indicate the points that represent TEM pictures shown in the figures with the same labels. For example, point 1A represents the picture shown in Figure 1A. The smaller letters, S, R, and B associated with the experimental points, represent spheres, rods, and bilayers (vesicles and lamellae) found under the experimental conditions. The points (circles or triangles) are the averages for the various morphologies of the aggregates and should be considered as rough estimates except for the primary spheres (represented by points 1A, 1C, and 2B).

As the pH* increases (see the upper scale), the average aggregation number first decreases (1E to 1C), then increases (1C to 1B), then decreases and increases again (1B to 1A to 2A), decreases once more (2A to 2B), and finally increases again (2B to 2C). Correspondingly, the average surface area per corona chain moves up and down, mirroring the variation in size. Clearly, the changes in both the average aggregation number and the average surface area per corona chain are complicated. Furthermore, the changes upon the addition of HCl (left) mirror those accompanying the addition of NaOH (right). Finally, it is worth noting that all spheres have similar aggregation numbers and similar surface areas per corona chain, as do all rods and all bilayers. The changes in the average values represent primarily changes in the relative frequency of those morphologies.

At point 1A in Figure 5, in the absence of any added microions, the aggregates are primary spheres with an average radius (r_{ave}) of 22 nm (see Figure 1A). The average aggregation number can be calculated from the sizes of the spheres using eq 2 and is found to be ca. 760. Correspondingly, the surface area per corona chain can be estimated using eq 3. The value is ca. 8.5 nm^2/chain and is thus relatively small, which suggests that the overall repulsive force among corona chains was also small when the aggregates were formed. The relatively small repulsion among corona chains is understandable. Because the P4VP corona block is nonionic, the intercorona repulsive force is provided only by the steric−solvation interaction; the latter is a short-range force and is relatively small. Another contributing factor which might be relevant to the morphology is the high value of the χ parameter between PS and P4VP blocks.[19]

From point 1A to 1B or from point 1A to 2A, the morphology changes from spheres alone to a mixture of spheres and rods. As the HCl or NaOH concentration increases from 400 nM to 40 μM (pH* = 11.8) or from 100 to 400 nM (pH* = 12.6), respectively, the relative fraction of rods increases, as seen from the dotted lines that connect the points for the various morphologies. The proximity of the experimental average (circle or triangle) to *R* indicates that rods predominate. Thus, the average aggregation number increases. Correspondingly, the average surface area per corona chain drops from ca. 8.5 to ca. 6 nm^2/chain. This means that the average repulsion among corona chains has decreased. Because the degree of ionization is low (α < 0.3%) in the concentration range used here, the electrostatic repulsion should not contribute much and the steric−solvation interaction still dominates the repulsion among corona. However, it is unlikely that such a small amount of HCl or NaOH can decrease the steric−solvation interaction alone and thus cause the morphological changes. Therefore, some other factors must contribute to the morphological changes, which we do not understand in detail.

As the concentration of HCl or NaOH increases further from point 1B to 1C or from point 2A to 2B, the morphology gradually shifts from the mixture of rods and spheres back to the spheres alone. The average aggregation number correspondingly decreases, and the average surface area per corona chain increases. This indicates that the average repulsive interaction

(19) Clarke, C. J.; Eisenberg, A.; Scala, J. L.; Rafailovich, M. H.; Sokolov, J.; Li, Z.; Qu, S.; Nguyen, D.; Schwarz, S. A.; Strzhemechny, Y.; Sauer, B. B. *Macromolecules* **1997**, *30*, 4188.

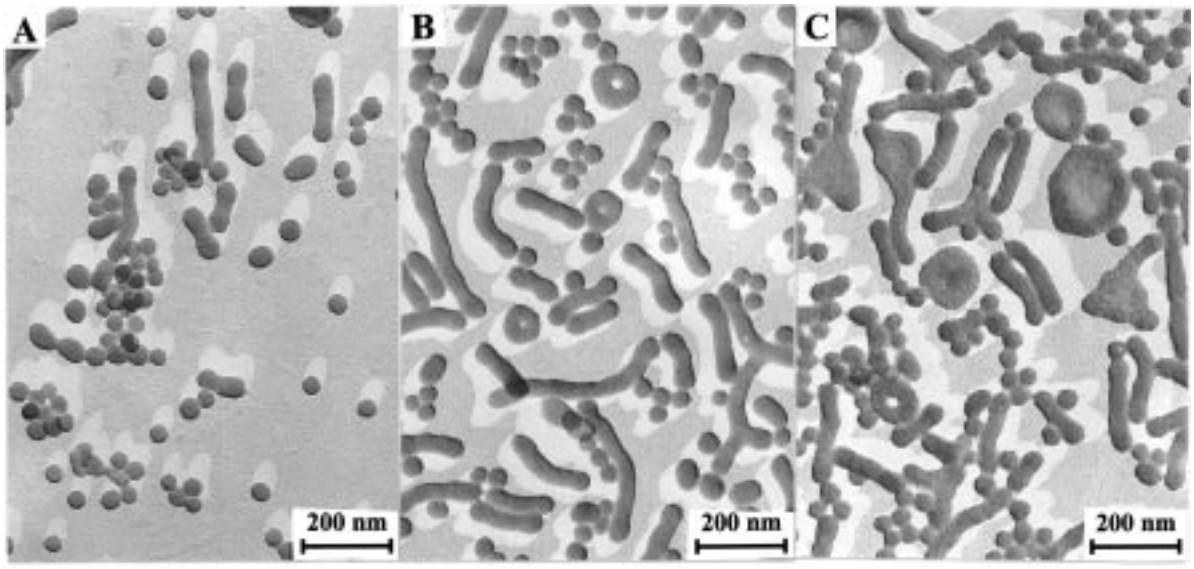

Figure 6. Effect of NaCl on the aggregate morphology of copolymer PS_{310}-*b*-$P4VP_{58}$: (A) 50 μM ($R = 0.004$); (B) 5.0 mM ($R = 0.36$); (C) 20 mM ($R = 1.43$).

among corona chains has increased. As the concentration increases to 5.0 mM at points 1C and 2B, the degree of ionization increases to ca. 32% and 2.5%, respectively (see Figure 4), and the unshielded electrostatic repulsion increases. The increase of the unshielded electrostatic repulsion dominates the corona repulsion, and thus spheres are seen at these points. In the same process, shielding and the decrease of the steric−solvation interaction are also operative because some of the acid or base remains unreacted in the solutions as a result of the presence of many simultaneous equilibria.

A further increase in the concentration of HCl or NaOH from point 1C to 1E or from point 2B to 2C results in a change of the aggregate morphologies from spheres to the mixture of morphologies. In the case of HCl, LCMs appear eventually. In the process, the average aggregation number increases and the average surface area per corona chain decreases again. This change indicates that the average repulsive force has decreased. The increased concentration of HCl or NaOH results in an increase of the degree of ionization from 32 to 88% or from 2.5 to 9.5%, respectively (see Figure 4). Again, multiple factors are operative; i.e., with increasing HCl or NaOH concentration, the unshielded electrostatic repulsion increases, the shielding increases, and the steric−solvation interaction decreases. However, in this case, the shielding effect becomes much more important. The degree of ionization obviously cannot increase beyond 100%. The addition of microions, however, can continue, thus increasing the shielding. Therefore, at relatively low concentrations of acid or base (concentrations below points 1C and 2B), the unshielded electrostatic repulsion is more important because of the low concentrations of free microions, but at high concentrations of acid or base (concentrations above points 1C and 2B), shielding dominates. Therefore, in that concentration range, the average repulsion among corona chains decreases.

There are many similarities between the acid effect and the base effect, which one can see from the near mirror image going from point 1A to point 1E or 2C, respectively. The major differences are found between the region from point 1C to point 1E (accompanying the increase of the HCl concentration from 5 to 20 mM) and the region from point 2B to point 2C (corresponding to a change of the NaOH concentration from 5 to 20 mM). At point 1E, we have LCMs, while at point 2C, we see a mixture of morphologies. The reason for the difference in the aggregation behavior can be ascribed to the fact that the empirical value of pK_b (20.5) is smaller than that of pK_a (22.7). At point 1E, the degree of ionization is ca. 88%, and thus the shielding is much stronger. At point 2C, the degree of ionization is ca. 9.5%, so the shielding is relatively weak. Since the shielding becomes dominant at relatively high concentrations (i.e., 20 mM), the coronae with high degrees of ionization collapse and LCMs appear. Thus, the average repulsion is much smaller at point 1E than that at point 2C. Correspondingly, the average surface area per corona chain obtained from experiments is ca. 3 nm^2/chain at point 1E and ca. 6.5 nm^2/chain at point 2C.

It is useful to compare the effects of HCl and NaOH seen here with those found in previous studies.[4] In the present study, a change in acid or base content to 40 μM HCl ($R = 0.003$) or 400 nM NaOH ($R = 3 \times 10^{-5}$) is sufficient to induce a morphological transition from spheres to rods with a small percentage of the spheres. In the previous study (PS_{420}-*b*-PAA_{10} in DMF/H_2O mixtures), 210 μM HCl ($R = 0.040$) was needed to change the morphology from spheres to rods, while 28 μM NaOH ($R = 0.005$) changed the aggregates from vesicles to spheres.[4] Thus the concentrations used here are much lower than those in the previous study. In that study, the concentrations ranged from 113 to 253 μM ($R = 0.04-0.09$) for the HCl effect and from 28 to 155 μM ($R = 0.005-0.02$) for the NaOH effect.[4] In the present study, the concentrations range from 400 nM to 20 mM ($R = 3 \times 10^{-5}$ to 1.43) for HCl and from 100 nM to 20 mM ($R = 7 \times 10^{-6}$ to 1.43) for NaOH. Thus the morphological effect extends over a broader concentration range in the present study. The reason for the difference in the morphological effect can be attributed to the amphiprotic properties of P4VP and small empirical values of pK_a and pK_b in DMF. Because both acids and bases can ionize the corona chains over a wide range of concentrations, the corona repulsion changes correspondingly. Thus, the overall morphology changes over a broader range of concentrations.

3.2. Effect of a Neutral Salt (NaCl) on the Aggregate Morphology of PS_{310}-*b*-$P4VP_{58}$. To see whether the pH* effect is truly due to the amphiprotic nature of P4VP in DMF, a neutral-salt effect (NaCl) on the aggregate morphology of the same copolymer was studied; the results are shown in Figure 6. With increasing NaCl content, the aggregates change from

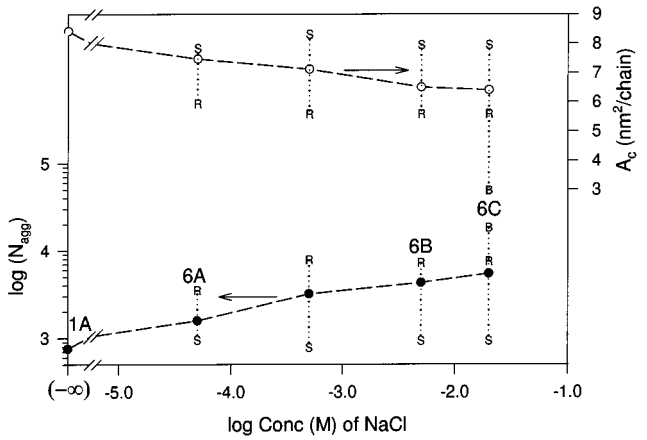

Figure 7. Plots of the logarithm of the average aggregation number (bottom plot and left axis label) and the average surface area per corona chain (top plot and right axis label) against the logarithm of the NaCl concentration in the solutions for aggregates of PS_{310}-*b*-$P4VP_{58}$. The $-\infty$ on the log Conc scale indicates zero microion concentration. Labels on the graph indicate the points that represent TEM pictures in the figures with the same labels. The small letters, S, R, and B, connected with points represent spheres, rods, and bilayers. The points are the averages of the aggregates and are rough estimates, except point 1A for primary spheres.

spheres (the starting point is Figure 1A) to rods or even lamellae. Figure 6A shows the appearance of a few rodlike aggregates at a NaCl concentration of 50 μM ($R = 0.004$). Figure 6B shows an increased number of rods along with some "doughnuts" and spheres at a concentration of 5.0 mM ($R = 0.36$). The rods, both straight and doughnut-shaped, have diameters similar to those of the spheres ($r = 22$ nm) in Figure 1A. When the NaCl concentration is increased to 20 mM ($R = 1.43$), the aggregates include lamellae, rods, doughnuts, and spheres, as shown in Figure 6C. Due to the limited solubility of NaCl in DMF, the concentrations could not be increased further.

Figure 7 gives the plot of the logarithm of the average aggregation number (bottom, label on left) and the average surface area per corona chain (top, label on right) against the logarithm of the NaCl concentration. Again, the $-\infty$ on the log Conc scale indicates zero microion concentration. As before, labels on the graph indicate the points that represent TEM pictures in the figures with the same labels. Again, the letters connected with points, S, R, and B, represent spheres, rods, and bilayers. The points are averages for the aggregates and should be considered as rough estimates, except for point 1A (primary spheres).

In contrast to the behavior of HCl or NaOH shown in Figure 5, there is only a very gradual change in average dimensions as the NaCl concentration changes. Rods start to appear at 50 μM (point 6A) and then become evident at 5 mM (point 6B); bilayers appear at 20 mM (point 6C). Over the whole range, the increase of the average aggregation number and the decrease of the average surface area per corona chain are monotonic. This reflects the progressive decrease of the average repulsive force among corona chains. Because the neutral salt cannot react with P4VP, the P4VP is still a nonionic block upon addition of NaCl. Thus the steric−solvation interaction, a short-range force, is the only source of the repulsion among corona chains. Since the addition of NaCl decreases the steric−solvation interaction, the average repulsion among corona chains decreases monotonically.

It is interesting to note that at 20 mM of NaCl (Figure 6C) and NaOH (Figure 2C) the range of morphologies (a mixture) and the average surface area per corona chain (ca 6.5 nm^2/chain) are quite similar. However, the nature of the NaCl effect differs from that of the NaOH effect. The NaCl effect is due purely to the decrease of the steric−solvation interaction; by contrast, many factors, such as an increase of unshielded electrostatic repulsion, an increase of shielding, and a decrease of the steric−solvation interaction, are operative for the NaOH effect.

3.3. Effect of the pH* on the Aggregate Morphology of PS_{600}-*b*-$P4VPMeI_{37}$. The next study is devoted to the pH* effect on the aggregate morphology of quaternized PS-*b*-P4VPMeI. The quaternization changes nonionic P4VP, to ionic $P4VPMe^+$, eliminates the basic properties from P4VP, and enhances the acidic properties. Thus, one may expect that shielding will be the most important factor influenced by the addition of HCl; however, multiple factors are still involved with added NaOH. Since preliminary results on PS_{310}-*b*-$P4VPMeI_{58}$ showed that the aggregates were too small ($r \approx 5$ nm) to be seen clearly by TEM, PS_{600}-*b*-$P4VPMeI_{37}$, containing a longer PS block and a shorter P4VPMeI block, was used in this study to increase the size of aggregates. The reason that the aggregates are so small is that the electrostatic repulsion is operative during the aggregation of quaternized copolymers.

3.3.1. Acid (HCl) Effect. Figure 8 shows the effect of HCl on the morphology of the aggregates of PS_{600}-*b*-$P4VPMeI_{37}$. Figure 8A shows the primary spherical aggregates of the copolymer without any added microions. The pH* is 7.3, decreased from 11.7 (of pure DMF) on the addition of the copolymer. One can see that the size ($r_{ave} = 8$ nm) of the aggregates is small when compared with the size of the spheres of nonquaternized PS_{310}-*b*-$P4VP_{58}$ ($r_{ave} = 22$ nm) shown in Figure 1A, despite the increase in the length of the PS block and the decrease in that of the corona-forming block. Upon addition of HCl to a total concentration of 2.0 mM ($R = 0.41$, pH* = 2.7), the size of the aggregates increases to $r_{ave} = 14$ nm, as shown in Figure 8B. With a further increase in the HCl concentration to 3.0 or 4.0 mM ($R = 0.61$ or 0.82; pH* = 2.4 or 2.3, respectively), the size of the aggregates increases significantly ($r_{ave} \approx 44$ or 190 nm) because the morphology changes to LCMs. This is seen in Figures 8C and 8D. It is interesting to note that rods and vesicles of this part of the phase diagram are bypassed because the regions either are too small or are completely eliminated.

3.3.2. Base (NaOH) Effect. The effect of NaOH on the morphology of aggregates of the same copolymer is shown in Figure 9. Figure 9A shows the significantly enlarged spheres ($r_{ave} = 22$ nm compared with the spheres in Figure 8A of 8 nm without any additives) at a NaOH concentration of 4.0 mM ($R = 0.82$, pH* = 11.0). The sizes of the aggregates are close to those of PS_{310}-*b*-$P4VP_{58}$ with nonionic corona shown in Figure 1A ($r_{ave} = 22$ nm). With an increase of the NaOH concentration to 5.0 mM ($R = 1.0$, pH* = 11.2), vesicular aggregates appear, as shown in Figure 9B. Figure 9C shows that when the NaOH concentration is increased to 7.0 mM ($R = 1.43$, pH* = 11.6), the aggregates change from vesicles back to spheres ($r_{ave} = 21$ nm). When the NaOH concentration is increased further to 10 mM ($R = 2.0$, pH* = 12.1), LCMs ($r_{ave} \approx 120$ nm) are formed, as shown in Figure 9D. Thus, this effect is similar to the effects of HCl and NaOH on aggregates of the nonquaternized copolymer PS_{310}-*b*-$P4VP_{58}$.

3.3.3. Semiquantitative Considerations. Figures 8 and 9 again show the complex pH* effect on the morphology of aggregates. As the pH* increases from 2.3 (at the highest acid content used here, corresponding to Figure 8D) to 7.3 (the neutral pH* of the quaternized copolymer solution, corresponding to Figure 8A) and then to 12.1 (Figure 9D), the aggregates

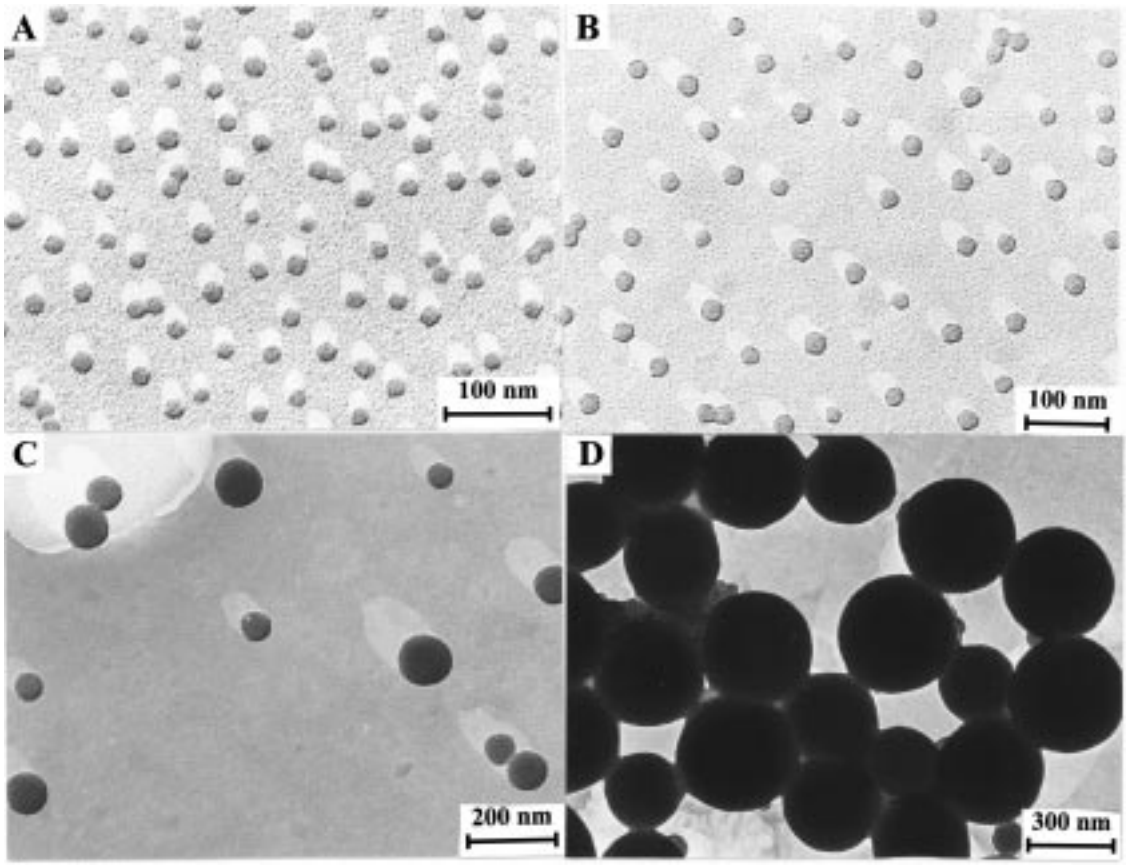

Figure 8. Effect of HCl on the aggregate morphology of copolymer PS_{600}-*b*-$P4VPMeI_{37}$: (A) without any added microions, pH* = 7.3; (B) 2.0 mM ($R = 0.41$), pH* = 2.7; (C) 3.0 mM ($R = 0.61$), pH* = 2.4; (D) 4.0 mM ($R = 0.82$), pH* = 2.3. The degrees of ionization for all samples are 100%.

gradually decrease their sizes from LCMs to small spheres at the neutral pH*, then change to vesicles, return back to spheres, and finally change back to LCMs again. A semiquantitative discussion of this pH* effect in terms of corona repulsive interactions is given below.

3.3.3.1. Polyprotic Properties of P4VPMeI in DMF. Scheme 2 shows the dissociation behavior of P4VPMeI in DMF. Once the P4VP block is quaternized to its ionic form (see structure **I** in Scheme 2), the basic site, N of the pyridine ring, is occupied. Due to the presence of the Me group on the pyridine ring, the α-H in structure **I** shows enhanced acidity.[14] In addition, after the release of the α-H in structure **I**, the *β*-H in structure **I** becomes the "α′-H" in structure **II**, which shows acidity too. However, after the release of one *β*-H in structure **I**, the H in structure **III** may not show acidity because the H joins the large resonance structure to stabilize structure **III**. Thus the copolymer is a polyprotic acid in DMF, and in contrast to the unquaternized P4VP, it no longer shows basic properties in that solvent.

The pH* measurements show that the α-H of $P4VPMe^+I^-$ ($pK_{a1} = 12.3$) is a relatively strong acid because, upon the addition of $P4VPMe^+I^-$, the pH* decreases from 11.7 of pure DMF to 7.3. The addition of NaOH to the $P4VPMe^+I^-$ solution in a stoichiometric amount increases the pH* from 7.3 to 11.4, still lower than the pH* of pure DMF. Under those conditions, the *β*-H in structure **I** is still an acid, since the added NaOH has converted structure **I** to structure **II**. Also the acidity of the *β*-H in structure **I** (pK_{a2} is ca. 20.3) is similar to that of the α-H of P4VP (pK_a is ca. 20.5). After release of one *β*-H, the second *β*-H in structure **I** cannot show its acidity for the same reason that the *β*-H of P4VP cannot show its acidity.

Additional evidence that $P4VPMe^+I^-$ can provide one *β*-H on the addition of NaOH comes from the UV−visible spectra. For 4VPMeI and similar structures, there is a well-defined charge-transfer peak.[20] The variation of the peak position as a function of the molar ratio of NaOH to 4VPMeI (R) is shown in Figure 10. One can see that, with increasing NaOH concentration, or *R* value, the peak shifts to higher wavelengths as *R* increases from 0 to 1 (accompanying the release of the α-H), then shifts back slightly when *R* increases from 1 to 2 (the release of the *β*-H), and finally reaches a constant value above an *R* value of 2 (the second *β*-H in structure **I** apparently is not released extensively). This peak position is a function of many factors, such as solvents and solute structures.[20] The addition of a small amount of NaOH (below 20 mM) does not change the properties of the solvent appreciably. Thus the change in the peak position can only be caused by a change of the structure of the repeat unit (see Scheme 2). This result is consistent with the results of pH* measurements.

In summary of the results of pH* measurements and the UV−visible spectra, one can conclude that $P4VPMe^+$ shows a two-step acidic dissociation. The addition of NaOH changes the nature of corona chains from cationic ($P4VPMe^+$) to nonionic (P4VPMe) and then to anionic ($P4VPMe^-$). The estimated degree of ionization is graphed in Figure 4 for the addition of NaOH. However, the addition of HCl cannot change the nature of the corona block.

3.3.3.2. Reasons for the pH* Effect on the Aggregate Morphology. Figure 11 shows the graph of the logarithm of the average aggregation number (lower curve, left axis) and the

(20) Kosower, E. M.; Skorcz, J. A. *J. Am. Chem. Soc.* **1960**, *82*, 2195.

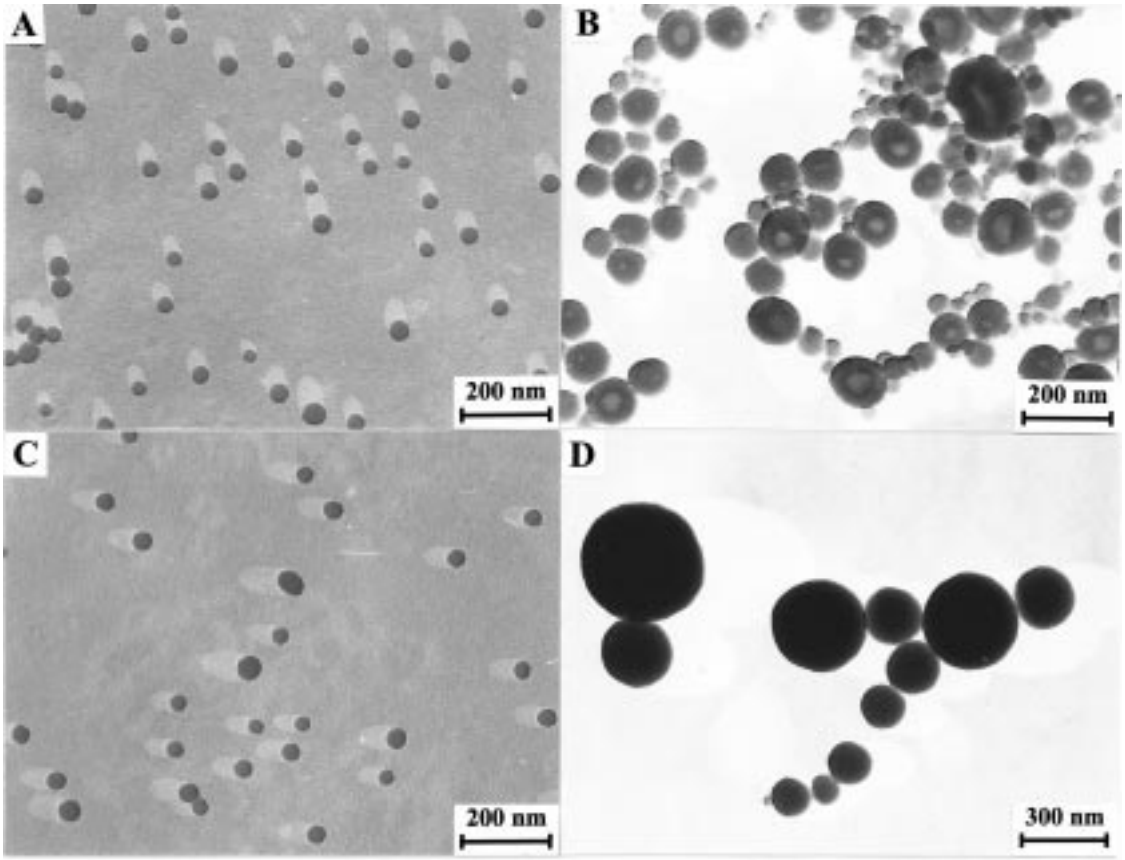

Figure 9. Effect of NaOH on the aggregate morphology of copolymer PS_{600}-*b*-$P4VPMeI_{37}$: (A) 4.0 mM ($R = 0.82$), pH* = 11.0, $\alpha = 18\%$; (B) 5.0 mM ($R = 1.02$), pH* = 11.2, $\alpha = 15\%$; (C) 7.0 mM ($R = 1.43$), pH* = 11.6, $\alpha = 36\%$; (D) 10 mM ($R = 2.04$), pH* = 12.1, $\alpha = 72\%$.

Scheme 2. Polyprotic Properties of P4VPMeI in DMF

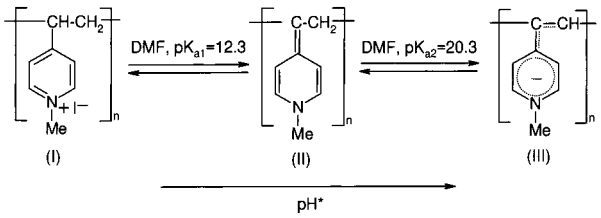

average surface area per corona chain (upper curve, right axis) against the logarithm of the microion concentration in the solutions. The upper scale gives the approximate value of pH*. As before, the $-\infty$ on the log Conc scale corresponds to a zero microion concentration and a pH* of 7.3. The effect of HCl is graphed on the left side (circles), while the effect of NaOH is graphed on the right side (triangles). Again, the labels on the graph indicate the points that represent TEM pictures shown in the figures with the same labels. The small letters S and B associated with point 8B represent the average sizes of the spheres and bilayers.

In the center of Figure 11, point 8A represents the small average aggregation number (ca. 25) and high average surface area per corona chain (ca. 38 nm^2/chain) for the aggregates formed without any additional microions. The low aggregation number and high surface area suggest that there is a large repulsive interaction among corona chains. This large repulsion mainly comes from the strong electrostatic repulsion, because the aggregates have completely ionized corona chains.

The acid effect (left side) is relatively straightforward. The changes seen here are similar to those of NaCl on aggregates of the nonquaternized copolymer PS_{310}-*b*-$P4VP_{58}$ but are more dramatic. As the HCl concentration increases from points 8A

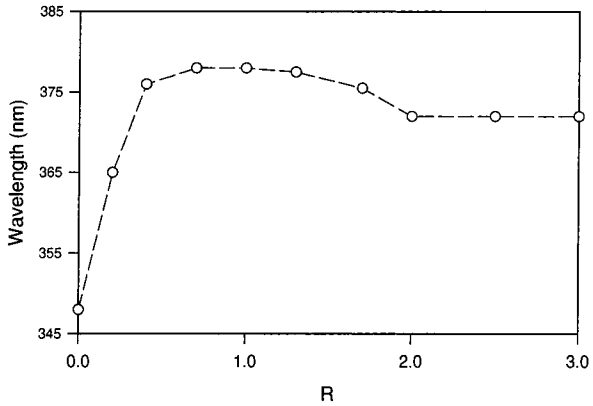

Figure 10. Plot of the wavelength of the charge-transfer peak from UV−visible spectra against the molar ratio of NaOH to 4VPMeI units (R).

to 8B, then to 8C, and finally to 8D, the average aggregation number increases monotonically and the average surface area per corona chain decreases correspondingly. This reflects the decrease of the repulsive force among corona chains. Since the corona chains are ionic, shielding is introduced upon addition of microions, which decreases the average electrostatic repulsion and, in a minor way, also the contribution of the steric−solvation interaction.

The base effect is more complex than the acid effect and is similar to the effect of HCl on aggregates of the nonquaternized copolymer PS_{310}-*b*-$P4VP_{58}$ (see Figure 5). Upon addition of NaOH (going from point 8A to points 9A and 9B in Figure 11), the average aggregation number increases and the average surface area per corona chain decreases. This indicates the decrease of the average repulsion among corona chains. As can

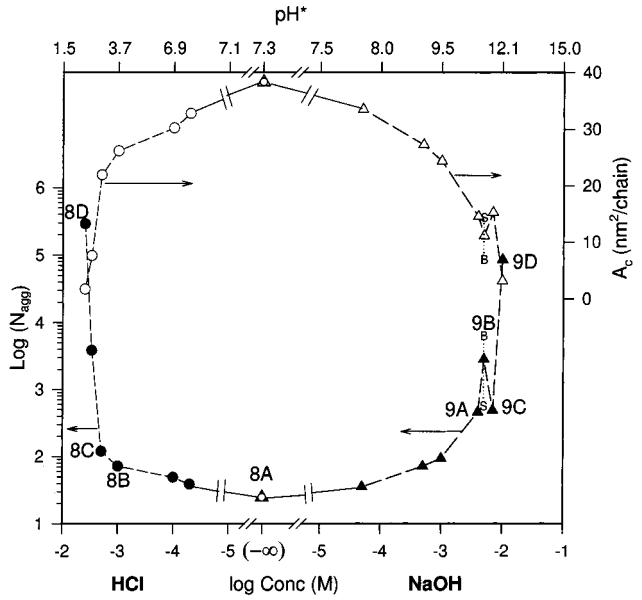

Figure 11. Plots of the logarithm of the average aggregation number (bottom plot and left axis label) and the average surface area per corona chain (top plot and right axis label) against the logarithm of the microion concentration in the solutions for aggregates of PS_{600}-*b*-$P4VPMeI_{37}$. The upper scale gives the approximate value of pH*. The $-\infty$ on the log Conc scale corresponds to a zero microion concentration and a pH* of 7.3. The effect of HCl is graphed on the left side (circles), while the effect of NaOH is graphed on the right side (triangles). The labels on the graph indicate the points that represent TEM pictures shown in the figures with the same labels. The small letters S and B connected with point 8B represent spheres and bilayers.

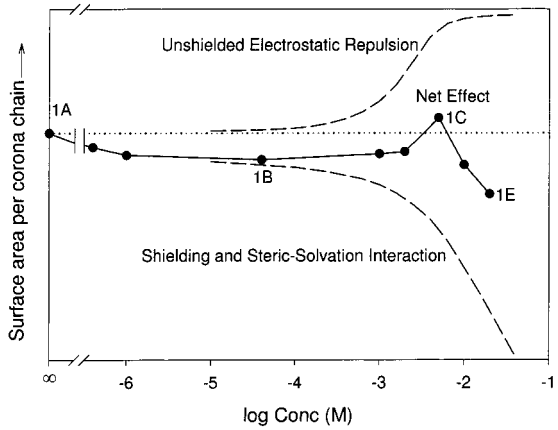

Figure 12. Illustration of the competition between unshielded electrostatic repulsion and shielding plus steric−solvation interaction.

be seen in Figure 4, as the NaOH concentration increases from 0 to 5 mM, the degree of ionization of the hydrophilic block decreases. Thus the decrease of the repulsion is mainly caused by the decrease of the electrostatic repulsion among the corona chains. As the NaOH concentration increases further from point 9B to point 9C (5 to 7 mM), the average aggregation number decreases and the average surface area per corona chain increases correspondingly, which reflects an increase of the repulsive interaction among the corona chains. This increase of the repulsion is electrostatic and is caused by the increase of the degree of ionization at NaOH concentrations above 5 mM (see Figure 4), which overcomes the increased shielding and the decrease of the steric−solvation interaction. With a further increase of the NaOH concentration to 10 mM from point 9C to point 9D, again, the average aggregation number increases and the average surface area per corona chain decreases. This indicates a decrease of the repulsion among corona chains, which, at this stage, is due to the dominance of shielding in the average repulsion.

It is useful to compare the aggregation behavior of quaternized PS_{600}-*b*-$P4VPMeI_{37}$ with that of the nonquaternized PS_{310}-*b*-$P4VP_{58}$. In the absence of added acid or base, the aggregates of the quaternized copolymer, with their ionic corona chains, have smaller sizes (r_{ave} = 8 nm) and thus a larger average surface area per corona chain (38 nm^2/chain) than those of nonquaternized copolymer (r_{ave} = 22 and 8.5 nm^2/chain, respectively). This shows that the electrostatic repulsion is far stronger than the steric−solvation interaction in the corona. Thus, at relatively high degrees of ionization, the electrostatic repulsion term dominates the overall repulsion. A much higher concentration of microions is needed for the morphological transition of the aggregates of the quaternized copolymer than for those of the nonquaternized system (i.e., several mM vs several μM for the nonquaternized copolymer). In addition, at both extremes, the aggregates of the quaternized copolymer can form LCMs and thus reach a low average corona−corona repulsion (reflected in the low values of A_c, ca. 2 nm^2/chain), which can be ascribed to the strong shielding effect in the presence of a high concentration of free microions. In the nonquaternized copolymer, LCMs are seen only upon the addition of high concentrations of HCl due to the high degree of ionization, but not for the NaOH addition.

3.4. Competition of Corona Repulsive Forces Contributing to the Net Effect. Because multiple factors (the unshielded electrostatic repulsion, the shielding, and the steric−solvation interaction) contribute to the overall result (i.e., the HCl effect on PS_{310}-*b*-$P4VP_{58}$), it would be useful if the contributions of these factors could be separated. Figure 12 attempts to separate these contributions which are illustrated by a schematic plot of the surface area per corona chain (A_c) against the logarithm of the microion concentration in solution. The symbols and the solid line indicate the total HCl effect on PS_{310}-*b*-$P4VP_{58}$, while the dotted line is the baseline and reflects the absence of any added microions. The dashed curve labeled "Unshielded Electrostatic Repulsion" reflects schematically those changes and is based on the plot of the degree of ionization versus the concentration (see Figure 4) because the unshielded electrostatic repulsion is obviously associated with the degree of ionization. The curve suggests that the unshielded electrostatic repulsion does not change much at low concentrations (i.e., below 10^{-4} M), then starts to increase dramatically after reaching a concentration of ca. 10^{-4} M, and finally reaches a plateau at high concentrations (i.e., above 10^{-2} M). The other dashed curve represents the increase of the shielding and the decrease of the steric−solvation interaction, which is based on the plot of the free microion concentration versus the overall microion concentration. Obviously, the corona repulsion decreases monotonically. At low concentrations (below point 1B), the corona repulsion decreases slowly, which is mainly due to the decrease of the steric−solvation force. At relatively high concentrations (above point 1B), the corona repulsion decreases more rapidly because the shielding joins the force balance. Thus, a competition emerges between the unshielded electrostatic repulsion and shielding along with the decrease of the steric−solvation interaction. As seen in Figure 12, at low concentrations (from point 1A to point 1B), the decrease of the steric−solvation interaction controls the aggregation process and drives the morphological changes. From point 1B to point 1C, the unshielded electrostatic repulsion contributes more and thus drives the changes of the aggregate morphology. However, the

unshielded electrostatic repulsion has its limit, while shielding continues as the increase of the free microion concentration. Eventually, from point 1C to point 1E, the shielding overcomes the unshielded electrostatic repulsion. Figure 12 should be considered only a qualitative representation of the competition, which attempts to show the trends.

This competition also applies to the effect of NaOH on the aggregate morphology of PS_{310}-*b*-$P4VP_{58}$. The same factors are operative. The degree of ionization increases slowly with increasing NaOH concentration; thus A_c increases less dramatically than it does in the case of HCl. The effects of shielding and the steric−solvation interaction are comparable in both cases and thus decrease A_c correspondingly. The result is similar to that of the HCl effect, as shown on the right side of Figure 5. However, LCMs do not appear due to the limited solubility of NaOH in DMF. The effect of NaOH on the aggregate morphology of PS_{600}-*b*-$P4VPMeI_{37}$ is more complicated. Below a concentration of 5 mM, the degree of ionization decreases with increasing concentration in that region (see Figure 4). All the factors reinforce each other; thus no competition takes place. Above a concentration of 5 mM, the degree of ionization starts to increase, so the competition begins. From that point on, we see a trend similar to that seen for the HCl effect on the aggregate morphology of PS_{310}-*b*-$P4VP_{58}$ (left side of Figure 11).

The competitive effects do not apply to the case of NaCl for nonquaternized PS_{310}-*b*-$P4VP_{58}$ or the case of HCl for quaternized PS_{600}-*b*-$P4VPMeI_{37}$. In both situations, the effects are purely due to the free microion concentration. However, the driving forces are different for these two effects. For the effect of NaCl on PS_{310}-*b*-$P4VP_{58}$, because of the nature of nonionic corona chains, the driving force is the decrease of the steric−solvation repulsive force. For the effect of HCl on PS_{600}-*b*-$P4VPMeI_{37}$, changes in shielding drive the morphology due to the completely ionic corona chains.

4. Conclusions

The changes of the morphology as a function of pH* for the PS-*b*-P4VP systems are very complex. Starting with a pH* of 7 (20 mM HCl), as the pH* increases to the neutral pH* of the nonquaternized polymer solution (12.3), the aggregates change from LCMs to a mixture of various morphologies, to small spheres, to rods, and back to small spheres at the neutral pH*. With increasing pH* (to 18 at 20 mM NaOH), the aggregate morphology changes to rodlike aggregates, then again to small spheres, and finally to a mixture of morphologies. This morphological complexity can be attributed to the amphiprotic properties of P4VP corona chains. Acids or bases can ionize the nonionic P4VP to cationic $P4VP^+$ or anionic $P4VP^-$ in DMF solutions. With increasing concentration of HCl or NaOH, the unshielded electrostatic repulsion increases, while shielding decreases the electrostatic repulsion and the steric−solvation interaction decreases correspondingly. Therefore, a competition is introduced between these two opposite driving forces. At low acid or base concentrations, the decrease of the steric−solvation interaction drives the morphological changes. At high acid or base concentrations, shielding is the main driving force. In between, the unshielded electrostatic repulsion takes over.

Adding NaCl to PS_{310}-*b*-$P4VP_{58}$ only decreases the steric−solvation interaction because a neutral salt cannot change the nonionic nature of PS-*b*-P4VP. Therefore, the morphology changes monotonically in the direction of spheres to rods and bilayers. The pH* effect on the aggregate morphology of the copolymer PS_{600}-*b*-$P4VPMeI_{37}$ was also examined. The HCl effect only increases shielding because the basic sites are occupied by the Me groups. Thus, the morphology only includes primary spheres and LCMs. The NaOH effect is more complex due to the two-step neutralization. In the first step (below 5 mM), with increasing NaOH concentration, all three factors (unshielded electrostatic repulsion, shielding, and the steric−solvation interaction) result in the decrease of the repulsive interaction among corona chains. Thus, the aggregates change from primary spheres to a mixture of vesicles and spheres. In the second step (above 5 mM), the competition starts between the unshielded electrostatic repulsion and shielding plus the steric−solvation interaction. Therefore, the aggregates change from a mixture of morphologies back to spheres and finally to LCMs.

Although the morphological effect of the added microions on block copolymer aggregates has been shown before,[4] this level of morphological complexity as a function of pH* has never been observed. In addition, the microion concentrations used here to induce the morphological transitions are extremely low, i.e., 100 nM NaOH or 400 nM HCl, which is again unprecedented. Therefore, the force balance, which is responsible for morphological changes in amphiphilic systems,[4] is much more delicate than has been appreciated before.

Acknowledgment. We thank the donors of the Petroleum Research Fund, administered by the American Chemical Society, and the NSERC of Canada for support of this work.

JA983712M